

On Modeling Satellite-to-Ground Path-Loss in Urban Environments

Akram Al-Hourani¹, Senior Member, IEEE, and Ismail Guvenc², Senior Member, IEEE

Abstract—We are currently witnessing a leap in provisioning wireless networks using satellites, enabled by the recent reduction in the launching costs and the advent of the Internet-of-Things. Understanding the path-loss between satellites and ground users is vital for the proper planning and design of such networks. This letter presents a systematic framework for modeling satellite-to-ground path-loss in urban environments. The modeling approach is semi-analytic, where the line-of-sight probability is obtained using tractable tools from stochastic geometry, while the shadowing is captured using a Gaussian mixture model that can be trained using measurements collected from global navigation satellite system (GNSS) receivers. The presented modeling framework balances simplicity and accuracy as illustrated with the results of the conducted measurements.

Index Terms—Satellite-to-ground, IoT-over-satellite, land mobile-satellite, GNSS, GPS, path-loss modeling, stochastic geometry.

I. INTRODUCTION

SPACE access is rejuvenated! Driven by the entrepreneurial efforts to improve space technologies, there has been a recent leap in satellite launch cost reduction, motivating many new players to enter the satellite communication industry. We are currently living in a world that is completely reliant on connectivity where satellites can provide the ultimate flexibility to complement the advancing terrestrial wireless services. For quite a long period, satellite connectivity was limited to a narrow range of applications, and was usually out-of-reach for many users due to cost and technology limitations. With the prospects of providing hybrid satellite-terrestrial services, a seamless coverage continuum can be created, not only to cover un-served remote regions but also to serve emerging machine-to-machine/Internet-of-things connectivity [1]. Hybrid satellite connectivity augments the reliability of terrestrial networks against natural disasters, physical attacks, and failures, in addition to patching intermittent black spots, and to cater for spikes in traffic demands.

In order to develop efficient satellite-to-ground (StG) wireless services, it is fundamental to understand the dynamics of the radio channel behavior between satellites and the underlying users. The importance of modeling efforts for StG has long been understood and many excellent measurement campaigns and research works have addressed different aspects of the modeling. Perhaps the crown of these studies are the works by the International Telecommunication Union (ITU) [2] on *land*

mobile-satellite channel, and the related work by 3GPP [1] to study the prospect of extending 5G services using *non-terrestrial networks*. Both of these investigations provide very relevant empirical channel models, where the emphasis on the uniqueness of propagation in urban environments. The shadowing, reflections and diffraction caused by buildings and structure add to the complexity of StG in these environments, as opposed to typical fixed-satellite links where the primary concerns are related to atmospheric and rain impairments. One of the earliest models for land mobile-satellite channel was provided in [3] which primarily captures the statistical processes of fading. Since then, many excellent works have been published including [4] and [5] among others. The recent advancement in unmanned aerial vehicles (UAV) technology has further enriched the modeling efforts of StG, because UAV-to-ground (also called air-to-ground [6]) models have a high resemblance to StG. Although ITU and 3GPP models are both built using certain set of empirical data, they do not offer tunability for local urban properties.

Since environment-specific properties strongly impact the radio propagation, the primary objective of this letter is to provide a systematic framework for rapidly constructing a custom StG path-loss model. The framework is tuned based on easy-to-obtain signal measurements from the Global Navigation Satellite System (GNSS) receivers. The benefits of the framework are three folds: (i) it allows tailoring its flexible parameters based on the local properties of the urban environment under study; (ii) it shows how these parameters could be easily tailored using GNSS receiver measurements without the need to resort for expensive lab-grade equipment; and (iii) the utilized Gaussian mixture distribution is widely adopted in both analytic and simulation approaches for performance prediction. These benefits are facilitated by the semi-analytic approach of the proposed framework, leveraging the recent works on tractable line-of-sight (LoS) probability [7] and the recent extensive UAV-to-ground empirical studies.

II. SATELLITE-TO-GROUND LOS PROBABILITY MODEL

Consider a satellite at a given time instant with a slant range (distance) d from an observer near to the ground level. The formed angle between the horizon and the line to the satellite is called the elevation angle and denoted by θ . The receiver is assumed to be located in built up region, as depicted in Fig. 1, either with an ideal hemispheric antenna pointed upward, or with the ability to steer the beam towards the satellite location. The former scenario is typically used for sensor-like applications operating at relatively low frequencies (such as the L/S-bands), while the beam steering, whether mechanical or electrical, might be required for higher directionality scenarios in the X-band and above.

Manuscript received October 14, 2020; accepted November 7, 2020. Date of publication November 16, 2020; date of current version March 10, 2021. The associate editor coordinating the review of this letter and approving it for publication was L. Mucchi. (Corresponding author: Akram Al-Hourani.)

Akram Al-Hourani is with the School of Engineering, RMIT University, Melbourne, VIC 3000, Australia (e-mail: akram.hourani@rmit.edu.au).

Ismail Guvenc is with the Department of Electrical and Computer Engineering, North Carolina State University, Raleigh, NC 27606 USA (e-mail: iguvenc@ncsu.edu).

Digital Object Identifier 10.1109/LCOMM.2020.3037351

1558-2558 © 2020 IEEE. Personal use is permitted, but republication/redistribution requires IEEE permission. See <https://www.ieee.org/publications/rights/index.html> for more information.

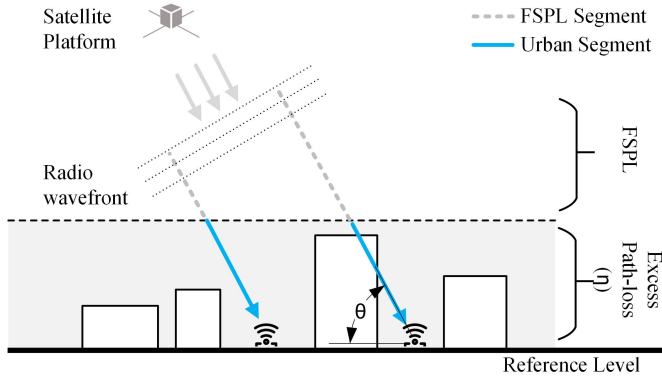


Fig. 1. Illustration of the planner radio wavefront indicating the two segments impacting satellite-to-ground propagation.

For such an urban environment, a general framework for the line-of-sight probability φ_{LoS} in built-up regions was originally developed in [7] for UAV applications. The framework is built based on stochastic geometry and it predicts φ_{LoS} between any two arbitrary points of heights h_1 and h_2 and a ground distance r as follows¹

$$\varphi_{\text{LoS}} = \exp \left(-2a \int_0^r G \left(\frac{x}{r} (h_2 - h_1) + h_1 \right) dx \right), \quad (1)$$

where $G(\cdot)$ is the complementary cumulative distribution function (CCDF) of the buildings heights, and a is a constant related to the geometry of the urban environment. In this model we select the use of Rayleigh distribution to capture the randomness in these heights as recommended by the ITU in [9]. Accordingly, we have

$$G(h) = \exp \left(-\frac{h^2}{2\sigma_b^2} \right), \quad (2)$$

where $\sigma_b = \mu_b \sqrt{2/\pi}$, and μ_b represents the mean of the buildings' heights. Solving the integral in (1) gives us the following closed-form expression,

$$\varphi_{\text{LoS}} = \exp \left(-\frac{a\sigma_b\sqrt{2\pi}}{h_2 - h_1} \left[\Phi \left(\frac{h_2}{\sqrt{2}\sigma_b} \right) - \Phi \left(\frac{h_1}{\sqrt{2}\sigma_b} \right) \right] r \right), \quad (3)$$

where $\Phi(\cdot)$ is the error function.

While the UAV links were considered in [7], StG channels require special treatment because of the significantly higher altitude of satellites when compared with UAVs. In the case of StG, the height h_2 is the distance between the satellite and the projection on the local horizontal plane; note that this is not the conventional satellite height which usually represents the distance from the satellite to its sub-point on the earth surface. Moreover, the distance r is between the observer and the projection on the local horizontal plane. These dimensions are illustrated in Fig. 2. Since the receiver's height is very close to the ground, we can have the approximations $\Phi \left(\frac{h_1}{\sqrt{2}\sigma_b} \right) \approx 0$ and $h_2 - h_1 \approx h_2$. Also, since the height of the satellite is very high when compared to σ_b , we have $\Phi \left(\frac{h_1}{\sqrt{2}\sigma_b} \right) \approx 1$.

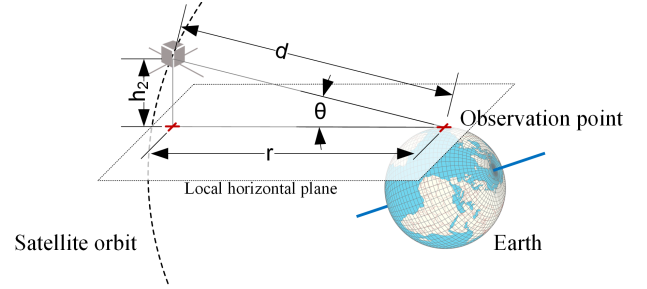


Fig. 2. The extension of the terrestrial LoS probability model in [7] to satellite scenarios, indicating the parameters used in (1) and (3).

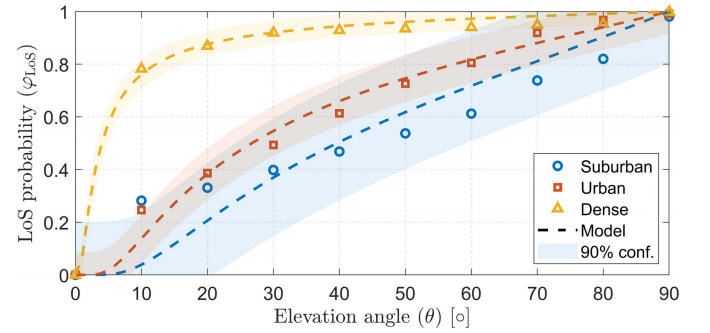


Fig. 3. The LoS probability based on the proposed model (5) compared with empirical measurements of 3GPP [1], the fit values are $\beta = \{0.57, 0.35, 0.048\}$ for suburban, urban, dense-urban scenarios respectively.

Thus, by substituting these in (3) we derive a simplified LoS probability as follows,

$$\varphi_{\text{LoS}} = \exp \left(-\beta \frac{r}{h_2} \right), \quad \text{where } \beta = a\sigma_b\sqrt{2\pi}. \quad (4)$$

It is much convenient to describe the LoS probability in terms of the elevation angle θ as follows:

$$\boxed{\varphi_{\text{LoS}} = \exp(-\beta \cot \theta)}. \quad (5)$$

This analytic model shows a good agreement with the collected line-of-sight (LoS) probabilities in 3GPP model [1] as depicted in Fig. 3, with a better fit in denser environments.

III. SATELLITE-TO-GROUND PATH-LOSS MODEL

The ionosphere roughly starts at around 1,000 km above the earth surface, and its influence on satellite radio signal is well-studied in the literature and by the ITU-R. Even though the ionosphere causes significant impairments to the radio signal (including Doppler, polarization rotation, scintillation, and group delay), its *absorption* for frequencies above 70 MHz is negligible [10]. On the other hand, attenuation due to *atmospheric* absorption has a measurable influence depending on the travelled distance by the signal, and this directly translates into dependency on the elevation angle θ . ITU has also laid a detailed model for obtaining the atmospheric absorption based on layered approximation of the atmosphere [11]. Based on the ITU model, we show in Fig. 4 the impacts of the frequency and the elevation angle on the atmospheric path-loss; the code was written in Matlab and is made available online [12]. This absorption occurs as an additive term to the satellite path-loss and denoted as L_A .

Looking at the journey of a microwave signal (1 to 30 GHz) from the satellite towards a ground receiver, we find that

¹This corresponds to equation (11) in [7], with an approximation in the upper limit as proven in [8].

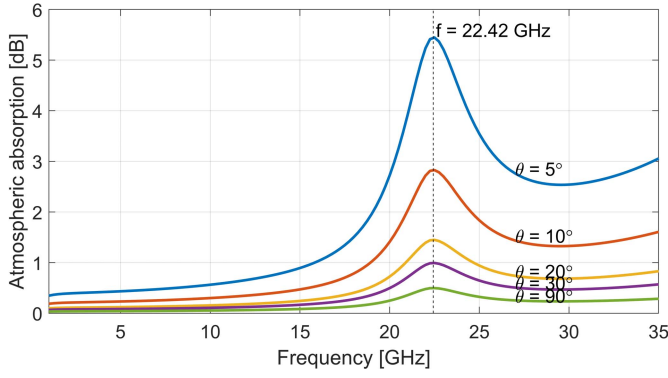


Fig. 4. Losses due to atmospheric absorption, constructed according ITU-R P.676-12-Annex 1 model using the International Standard Atmosphere model for pressure and temperature profiles, and standard vapor profile by ITU-R P.835-2 model. The vertical line represents water vapor absorption band.

the vast majority of the propagation occurs in a free space segment, except the atmospheric absorption that needs to be accounted for. However, at the bottom layer of propagation, a major change in the propagation condition occurs due to the interactions with the near-surface urban structures (termed as *clutter*). As indicated in Fig. 1, the effect of the last segment can be captured as an additional path-loss quantity, called the *excess path-loss* in [13] and denoted as η , the same concept is adopted by 3GPP. The excess path-loss is typically modelled as a Gaussian mixture model (GMM) having two components that correspond to the LoS and the non-LoS (NLoS) propagation conditions. Thus, the distribution is modelled as:

$$\eta(\theta) \sim \varphi_{\text{LoS}} \mathcal{N}(\mu_{\text{LoS}}, \sigma_{\text{LoS}}^2) + (1 - \varphi_{\text{LoS}}) \mathcal{N}(\mu_{\text{NLoS}}, \sigma_{\text{NLoS}}^2), \quad (6)$$

where the component mixture ratio is the angle-dependent LoS probability $\varphi_{\text{LoS}}(\theta)$. The mean μ_{ξ}^2 and standard deviation σ_{ξ} depend on the propagation mode $\xi = \{\text{LoS}, \text{NLoS}\}$. The standard deviation usually shows very weak dependency on the elevation angle [1], [13], with variations no more than ± 1 dB in dense-urban scenarios, and much lower variations in urban scenarios. In order to conserve the simplicity, and yet a good degree of accuracy, we propose to capture both the mean and the standard deviation as angle independent. This assumption will show to hold well in the experimental results presented in Section VI. Accordingly, the StG path-loss is given by,

$$\text{PL}(d, \theta) = \text{FSPL}(d, f) + L_A(f, \theta) + \eta(\theta), \quad (7)$$

where $\text{FSPL}(d, f)$ is the free space path-loss,

$$\text{FSPL}(d, f) = 20 \log_{10}(f) + 20 \log_{10}(d) - 147.55, \quad (8)$$

where f is the carrier frequency in Hz and d is the radio distance to the satellite in meters.

IV. EXTRACTING MODEL PARAMETERS

In order to build the excess path-loss model in (6), we need to extract the five parameters $\mathbf{x} = \{\beta, \mu_{\text{LoS}}, \sigma_{\text{LoS}}, \mu_{\text{NLoS}}, \sigma_{\text{NLoS}}\}$ from empirical measurements.

²Mean value of the excess path-loss μ is called *clutter loss* in 3GPP model and in ITU-R P.2402-0.

These parameters can be estimated using statistical good-of-fit methods because the target quantity, i.e. η , is a random variable. There are several methods for statistical distribution fitting, however we know that the distribution of η is conditional on the probability of LoS φ_{LoS} which in turn is deterministically calculated based on the elevation angle θ . Accordingly, we can not simply group all measurements into a single bucket and try to fit their distribution directly using general statistical good-of-fit methods.

Alternatively, we could extend known statistical good-of-fit measures such as the *Kolmogorov-Smirnov (KS) statistic* to include the deterministic LoS condition. Let the conditional cumulative distribution function (CDF) of the excess path-loss be denoted as $F_{\eta}(u|\theta, \mathbf{x})$ and the empirical CDF of the collected measurements (samples) as $F_s(u|\theta)$, where s denotes the *samples*. Then, we define the conditional KS-statistic as:

$$D(\theta, \mathbf{x}) = \max |F_s(u|\theta) - F_{\eta}(u|\theta, \mathbf{x})|, \quad (9)$$

which directly stems from the definition of the conventional KS-statistic [14]. Note that since $F_{\eta}(u|\theta, \mathbf{x})$ is a GMM, then its CDF is the weighted sum of the two Gaussian components CDFs:

$$F_{\eta}(u|\theta, \mathbf{x}) = 1 + \frac{1}{2} \left[\varphi_{\text{LoS}}(\theta) \Phi \left(\frac{u - \mu_{\text{LoS}}}{\sigma_{\text{LoS}} \sqrt{2}} \right) + (1 - \varphi_{\text{LoS}}(\theta)) \Phi \left(\frac{u - \mu_{\text{NLoS}}}{\sigma_{\text{NLoS}} \sqrt{2}} \right) \right]. \quad (10)$$

The empirical CDF of the measurements can be obtained by binning the samples into N discrete groups of elevation angles, where the bin size is $\Delta\theta = 90^\circ/N$, and the center of the bin is denoted as $\theta_n = (n - 1/2)\Delta\theta$, where $n \in [1, N]$ is the bin index. The overall good-of-fit is then obtained as the sum of all bins' individual good-of-fit, and thus the optimal parameter vector can be found as follows:

$$\mathbf{x}^* = \arg \min_{\mathbf{x}} \left[\sum_{n=1}^N \max |F_s(u|\theta_n) - F_{\eta}(u|\theta_n, \mathbf{x})| \right]. \quad (11)$$

As this objective function is nonlinear and stochastic, we can effectively employ the Genetic Algorithm (GA) for obtaining the optimal vector \mathbf{x}^* .

Binning the samples into larger bins, i.e. smaller N , would lead to richer *per-angle* distribution; however, it might also degrade the availability of samples for estimating the LoS probability. On the other hand, having granular bins might cause poorer per-bin distribution estimate and thus poorer overall fitting. In order to resolve this, we define a *hyper cost function* by evaluating the fitness of the model's standard deviation with respect to the samples' moving standard deviation $\tilde{\sigma}_s$, as follows:

$$J = \sqrt{\frac{1}{K} \sum_{k=1}^K [\tilde{\sigma}_s(\theta_k) - \sigma(\theta_k)]^2}, \quad (12)$$

where k represents the sample index and K is the total number of samples. Since the model uses GMM, the variance for a given θ is obtained as

$$\sigma^2(\theta_n) = \varphi_{\text{LoS}} \sigma_{\text{LoS}}^2 + \varphi_{\text{NLoS}} \sigma_{\text{NLoS}}^2 + \varphi_{\text{LoS}} \varphi_{\text{NLoS}} (\mu_{\text{LoS}} - \mu_{\text{NLoS}})^2, \quad (13)$$

where the $\varphi_{\text{NLoS}} = 1 - \varphi_{\text{LoS}}$ which is calculated from (5). The optimal number of bins could then be optimized such that,

$$N^* = \arg \min_N [J]. \quad (14)$$

We illustrate in Section VI the impact of the data set size on the optimal number of bins.

V. DATA COLLECTION USING GNSS RECEIVERS

Getting practical measurements for a wide range of elevation angles is not a straightforward task, because a geostationary satellite will have a fixed elevation angle in a certain geographic region. A low-earth-orbit constellation could be used for such a task, but will pose some challenges in constructing specialized receiver for measuring the received signal level. On the other hand, someone could exploit the ubiquity of the GNSS receivers for collecting signal strength samples. GNSS receiver modules report a plethora of information in addition to the geographic coordinates and time, and they can be easily mounted for rapid satellite channel modeling. Reported GNSS information already include the elevation angle θ estimate, and the carrier-to-noise power spectral density ratio C/N_o . In order to capture this information we need to distill the standard NMEA messages,³ in particular the GPGSV frame that reports detailed information about the satellites in view. The GPGSV frame can be converted into a list of available satellites with the corresponding elevation angle and signal quality C/N_o .

A simple measurement setup as illustrated in Fig. 6 could be used, composed of a USB GNSS (or GPS) module connected to a logging device, e.g. laptop running a Matlab/Python script, or any generic logging software. The data could be stored in a local drive in table format containing: time stamp, longitude, latitude, altitude, elevation angle, C/N_o , and satellite GPS number (PRN). In order to obtain the distance d to the satellite we can use the Simplified Perturbations Model Algorithm (SGP-4) which gives sufficient accuracy for the near-circular orbits GPS satellites. The orbital parameters are extracted based on the collected satellite PRN. For converting the measured C/N_o into useful channel measurements we first need to formulate the link budget of a typical GPS satellite. The received power in dBm is formulated as follows,

$$P_r = P_t + G_t + G_r - \text{PL}, \quad (15)$$

where P_t is the satellite transmit power, while G_t, G_r are the antenna gain of the satellite and the GNSS receiver, respectively. The equivalent isotropic radiated power (EIRP), i.e., $\text{EIRP} = P_t + G_t$, value is not actually a constant and it depends on many factors such as the GPS satellite generation, satellite antenna pattern, and boresight/elevation angles. Previous measurements of these variations showed fluctuations in the order of ± 1 dB [15].

Recalling our aim to tune the proposed model based on the underlying urban environment, we do not account for the variability in the EIRP, since the expected shadowing variations significantly exceed EIRP fluctuations, especially

³National Marine Electronics Association.

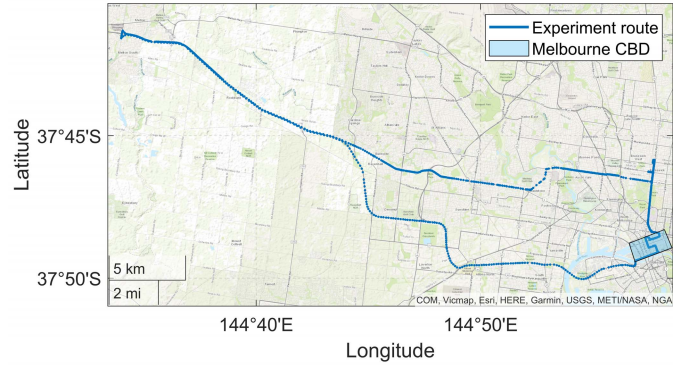


Fig. 5. The route of the vehicle during samples collection.

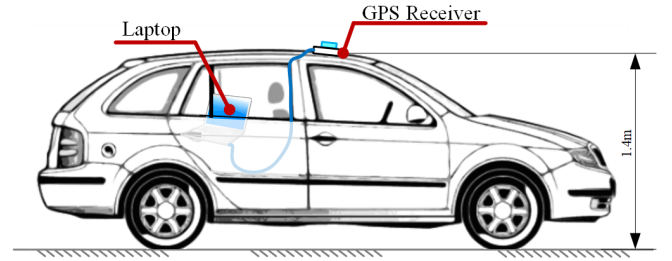


Fig. 6. The setup of the experiment for tuning StG path-loss model using GNSS satellites power measurements.

for NLoS. The received signal power is therefore related to the reported C/N_o as follows:

$$P_r = [C/N_o]_{\text{dB}} + N_o, \quad (16)$$

where N_o is the noise power spectral density. By substituting (7) and (16) into (15) and re-arranging, we get

$$\eta = -[C/N_o]_{\text{dB}} - \text{FSPL} - L_A + g_r + \gamma, \quad (17)$$

where $\gamma = P_t + G_t - N_o + G_{r_o}$ is treated as a constant. Note that we have split the receiver antenna gain into the maximum gain component G_{r_o} and the normalized angle-dependent directivity component g_r which can be obtained from typical GNSS patch antenna datasheets. The atmospheric losses L_A in the L-band are rather negligible; however, we choose to calculate this known quantity using the method described in Section III. Calibrating the system is done by obtaining the value of γ in (17). This is achieved by calculating the mean excess path-loss at the highest available elevation angle in the data set (for example $\geq 75^\circ$) and then adjusting γ such that $\bar{\eta}(\geq 75^\circ)$ is forced to zero, because it is expected to have a negligible excess path-loss at these high elevation angles.

VI. NUMERICAL RESULTS

The aim of this experiment is to serve as a numeric example and to demonstrate the ability of the proposed framework to rapidly estimate the StG path-loss parameters. We follow the simple experimental setup as depicted in Fig. 6 to collect GPS signal quality $[C/N_o]_{\text{dB}}$ and we process the data as indicated in Section V. The experiment route is depicted in Fig. 5, where the vehicle is predominantly driven in a range of typical suburbs of Melbourne metropolitan area. The relation in (17) is used to calculate the excess path-loss where the elevation angle θ is obtained using SGP-4 algorithm based on the satellite

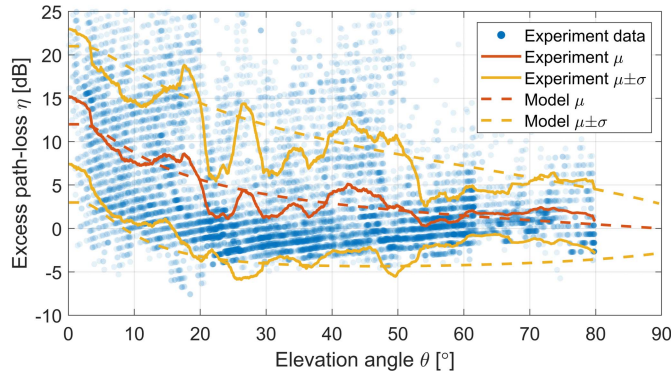


Fig. 7. The results of the proposed modeling framework fitted to the collected measurements from the GPS receiver. The parameter vector is $\{\beta = 2.3, \mu_{\text{LoS}} = 0 \text{ dB}, \sigma_{\text{LoS}} = 2.8 \text{ dB}, \mu_{\text{NLoS}} = 12 \text{ dB}, \sigma_{\text{NLoS}} = 9 \text{ dB}\}$.

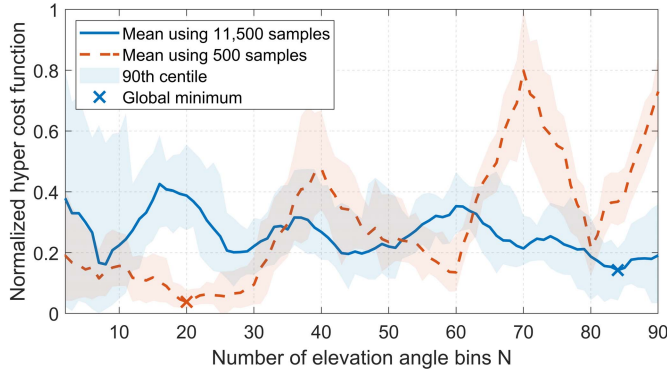


Fig. 8. The impact of the number of bins on the hyper cost function.

PRN number and the current coordinates of the vehicle. The unknown parameter γ is calibrated based on the reasonable assumption that the mean of η is zero for $\theta \geq 75$.

The collected samples for the excess path-loss are depicted in Fig. 7 as a density plot of discrete points, along with their moving average and moving standard deviation (with filter size of 500 points). It is worth to mention that the total recording time of the experiment is approximately 3:15 hours, with a total of $\approx 11,500$ samples, i.e. the sampling rate is around 1 Hz. Fig. 7 indicates a good match with the model's per θ mean and standard deviation where the RMSE error is 1.6 dB for the mean line and 2.1 dB for the standard deviation. The figure uses the model variance formula as given in (13) and the model mean formula as the sum of GMM components weighted with the probability of LoS:

$$\mu = \varphi_{\text{LoS}} \mu_{\text{LoS}} + (1 - \varphi_{\text{LoS}}) \mu_{\text{NLoS}}. \quad (18)$$

In order to visualize the impact of the sample size on the optimal number of bins N^* , we depict in Fig. 8 the average hyper cost function for 10 optimization runs in two cases; (i) taking the full collected 11,500 samples, and (ii) randomly thinning the data down to 500 samples. As expected, the optimal N^* was lower when training the model with the smaller data set.

VII. CONCLUSION

This letter presented a parametric, yet accurate modeling framework for characterizing satellite-to-ground excess path-loss in urban environments. The framework is constructed using tractable tools from stochastic geometry to capture the line-of-sight probability, and it builds on the widely-used empirical UAV-to-ground channel model. We demonstrated that the proposed framework can be tuned easily by using measurements collected from commercially available GNSS receivers. The presented results show a good match between the excess path-loss obtained from measurements and the proposed model for a wide range of elevation angles, and can thus be conveniently used in future analytical studies.

REFERENCES

- [1] *Study on New Radio (NR) to Support Non Terrestrial Networks (Release 15)*, 3rd Generation Partnership Project, Technical specification group radio access network, 3GPP, document TR 38.811, 2018.
- [2] *Propagation Data Required for the Design of Earth-Space Land Mobile Telecommunication Systems*, International Telecommunication Union (ITU), P Series document ITU-R P.681-6, 2019.
- [3] C. Loo, "A statistical model for a land mobile satellite link," *IEEE Trans. Veh. Technol.*, vol. 34, no. 3, pp. 122–127, Aug. 1985.
- [4] A. Abdi, W. C. Lau, M. Alouini, and M. Kaveh, "A new simple model for land mobile satellite channels: First- and second-order statistics," *IEEE Trans. Wireless Commun.*, vol. 2, no. 3, pp. 519–528, May 2003.
- [5] S. Scalise, H. Ernst, and G. Harles, "Measurement and modeling of the land mobile satellite channel at ku-band," *IEEE Trans. Veh. Technol.*, vol. 57, no. 2, pp. 693–703, Mar. 2008.
- [6] W. Khawaja, I. Guvenc, D. W. Matolak, U.-C. Fiebig, and N. Schneckenburger, "A survey of Air-to-Ground propagation channel modeling for unmanned aerial vehicles," *IEEE Commun. Surveys Tuts.*, vol. 21, no. 3, pp. 2361–2391, 3rd Quart., 2019.
- [7] A. Al-Hourani, "On the probability of Line-of-Sight in urban environments," *IEEE Wireless Commun. Lett.*, vol. 9, no. 8, pp. 1178–1181, Aug. 2020.
- [8] A. Al-Hourani, "Interference modeling in low-altitude unmanned aerial vehicles," *IEEE Wireless Commun. Lett.*, vol. 9, no. 11, pp. 1952–1955, Nov. 2020.
- [9] *Propagation Data and Prediction Methods Required for the Design of Terrestrial Broadband Radio Access Systems Operating in a Frequency Range From 3 to 60 GHz*, International Telecommunication Union (ITU), M Series document ITU-R P.1410-5, 2012.
- [10] *Ionospheric Propagation Data and Prediction Methods Required for the Design of Satellite Services and Systems*, International Telecommunication Union (ITU), P Series document ITU-R P.531-11, 2012.
- [11] *Attenuation by Atmospheric Gases and Related Effects*, International Telecommunication Union (ITU), P Series, Radiowave propagation, document ITU-R P.676-12, 2019.
- [12] A. Al-Hourani, (2020). *Atmospheric Absorption Loss for Satellite Communications*. MATLAB Central File Exchange. [Online]. Available: <https://www.mathworks.com/matlabcentral/fileexchange/78865-atmospheric-absorption-loss-for-satellite-communications>
- [13] A. Al-Hourani, S. Kandeepan, and A. Jamalipour, "Modeling air-to-ground path loss for low altitude platforms in urban environments," in *Proc. IEEE Global Commun. Conf.*, Dec. 2014, pp. 2898–2904.
- [14] A. N. Pettitt and M. A. Stephens, "The kolmogorov-smirnov Goodness-of-Fit statistic with discrete and grouped data," *Technometrics*, vol. 19, no. 2, pp. 205–210, May 1977.
- [15] T. Wang, C. Ruf, B. Block, and D. McKague, "Characterization of the transmit power and antenna pattern of the GPS constellation for the CYGNSS mission," in *Proc. IGARSS - IEEE Int. Geosci. Remote Sens. Symp.*, Jul. 2018, pp. 4011–4014.